High-Precision Quantum Thermochemistry on Nonquasiharmonic Potentials: Converged Path-Integral Free Energies and a Systematically Convergent Family of Generalized Pitzer–Gwinn Appr…

ARTICLE *in* THE JOURNAL OF PHYSICAL CHEMISTRY A · DECEMBER 2005

Impact Factor: 2.69 · DOI: 10.1021/jp051742n · Source: PubMed

3 AUTHORS, INCLUDING:

Steven L Mielke
University of Minnesota Twin Cities
67 PUBLICATIONS **2,857** CITATIONS
SEE PROFILE

Donald Truhlar
University of Minnesota Twin Cities
1,342 PUBLICATIONS **81,158** CITATIONS
SEE PROFILE

High-Precision Quantum Thermochemistry on Nonquasiharmonic Potentials: Converged Path-Integral Free Energies and a Systematically Convergent Family of Generalized Pitzer−Gwinn Approximations

Vanessa Audette Lynch,[†] Steven L. Mielke,*[,‡] and Donald G. Truhlar*[,†]

Department of Chemistry and Supercomputer Institute, University of Minnesota, 207 Pleasant Street S.E., Minneapolis, Minnesota 55455-0431, and Department of Chemistry, Northwestern University, Evanston, Illinois 60208-3113

Received: April 5, 2005; In Final Form: August 22, 2005

Accurate quantum mechanical (QM) vibrational−rotational partition functions for HOOD, D_2O_2, $H^{18}OOH$, $H_2{}^{18}O_2$, $D^{18}OOH$, and $H^{18}OOD$ are determined using a realistic potential energy surface for temperatures ranging from 300 to 2400 K by using the TT-FPI-ESPE path-integral Monte Carlo method. These data, together with our prior results for H_2O_2, provide benchmarks for testing approximate methods of estimating isotope effects for systems with torsional motions. Harmonic approximations yield poor accuracy for these systems, and although the well-known Pitzer−Gwinn (PG) approximation provides better results for absolute partition functions, it yields the same results as the harmonic approximation for isotope effects because these are intrinsically quantal phenomena. We present QM generalizations of the PG approximation that can provide high accuracy for both isotope effects and absolute partition functions. These approximations can be systematically improved until they approach the accurate result and converge rapidly. These methods can also be used to obtain affordable estimates of zero-point energies from accurate partition functions—even those at relatively high temperatures.

1. Introduction

Obtaining accurate thermodynamic information about systems with highly anharmonic motions such as torsions is a challenging problem, and many methods have been proposed[1−32] to deal with this difficulty. Even evaluating the efficacy of these approximations is a challenging task because very few accurate benchmarks exist to which results of these methods may be compared. H_2O_2 is a particularly challenging system, where methods such as second-order perturbation theory[4] are known[33] to be inaccurate. In the present study, we extend our recent work on H_2O_2 by providing accurate quantum mechanical (QM) partition functions for all six isotopologs that result from replacing one or two atoms with their most common isotopic replacements (D or ^{18}O). The extent to which the approximate methods reproduce the trends of isotopic substitution should serve as a sensitive measure of their reliability.

Path-integral Monte Carlo methods provide an attractive scheme for obtaining accurate QM partition functions. In these methods, the low-frequency motions, which are usually those with the highest degree of anharmonicity, are typically the easiest to treat, both because these coordinates are easier to sample (i.e., have lower sampling variances) and because a smaller number, P, of path expansion parameters is needed in these coordinates than for those with high-frequency motions. Miller and Clary[27,28] have advocated a "torsional path-integral method" in which the difficult-to-treat high-frequency coordinates are treated as rigid, and this makes tractable the treatment of a relatively large number of floppy coordinates. An alternative approximation philosophy is to treat all the degrees of freedom within the accurate path-integral formalism, but use path expansions that are only sufficient to accurately handle the low-frequency motions, and then adjust the results in an approximate fashion. The well-known Pitzer−Gwinn (PG) method[3] may be considered one of the simplest approximation methods within this philosophy, because it employs a path-integral simulation for all degrees of freedom (albeit with $P = 1$, where $P = 1$ corresponds to the classical limit) and adjusts this based on a QM harmonic treatment. The PG method has already been shown to be substantially more accurate than the harmonic approximation for estimating absolute partition functions,[14] although it can do no better than the harmonic approximation for isotope ratios. In this article we will consider quantum mechanical generalizations of the PG scheme that employ path-integral simulations with $P > 1$. These new approximations converge to the accurate result in the limit of large P, and we will show that they converge much more rapidly than the accurate path-integral methods—in some cases yielding converged results even for $P = 2$ or 3. We also show how these methods can be used to obtain affordable estimates of the accurate zero-point energies.

2. Path-Integral Theory

The path-integral expression for the quantum mechanical internal (vibrational−rotational) partition function of a molecule is[34,35]

$$Q(T) = \int_S \mathrm{d}\mathbf{x} \oint \mathbf{D}[\mathbf{x}(s)] \exp\left(-\frac{1}{\hbar} A[\mathbf{x}(s)]\right) \qquad (1)$$

where $\hbar$ is Planck's constant divided by 2π, $\oint \mathbf{D}[\mathbf{x}(s)]$ is the integral over all closed paths $\mathbf{x}(s)$ of time duration $i\beta\hbar$ whose centroid position occurs at $\mathbf{x}$, β is $1/k_BT$, k_B is Boltzmann's

* Authors to whom correspondance should be addressed. E-mail: slmielke@chem.northwestern.edu; truhlar@chem.umn.edu.
[†] University of Minnesota.
[‡] Northwestern University.

10.1021/jp051742n CCC: $30.25
Published on Web 10/14/2005

constant, T is temperature, s is the distance along the path, and $A[\mathbf{x}(s)]$ is the action integral of path $\mathbf{x}(s)$ and is given by the expression

$$A[\mathbf{x}(s)] = \int_0^{\beta\hbar} \mathrm{d}s \left(\frac{\mu}{2} \left(\frac{\mathrm{d}\mathbf{x}}{\mathrm{d}t} \right)^2 + V(\mathbf{x}) \right) \tag{2}$$

where μ is the reduced mass of the system, and $V(\mathbf{x})$ is the potential energy at point $\mathbf{x}$. The S subscript under the integral in eq 1 indicates that the integration is only over distinguishable elements of phase space. In the present application, we adopt an equivalent approach of integrating over all space and dividing by σ^{sym}, the symmetry number of the system.[36,37]

Fourier path-integral (FPI) methods[31,34,35,38−57] represent the deviations of the paths from free-particle paths by a Fourier expansion. The conventional approach to FPI calculations truncates the infinite Fourier series to K terms, and the results converge as $O(1/K)$. A more efficient approach, introduced by Coalson,[41] that also uses a finite expansion but additionally uses a K-dependent rescaling of the Fourier coefficients results in $P = K + 1$ evenly spaced points on the paths being distributed as they would be in an infinite-dimensional Fourier expansion. Coalson[41] showed that if quadratures over such paths are evaluated using a P-point trapezoidal rule, the method is isomorphic to the widely used trapezoidal Trotter discretized path-integral scheme. We refer to this as the trapezoidal Trotter FPI (TT-FPI) method. Partition function estimates obtained via TT-FPI converge as $O(1/P^2)$. We have recently shown[58] that using the TT-FPI approach allows one to construct lower-order path-integral estimates at essentially no additional cost and that these estimates, called $Q^{[P]}_{\mathrm{TT-FPI}}$, display regular convergence that permits highly accurate extrapolation to the infinite-P limit.

The extrapolation of the path-integral results to the infinite-P limit is carried out by the enhanced same-path extrapolation (ESPE) approach,[58] which involves fitting the TT-FPI partition function values for the highest three available values of P (we use $P^{\max}$, $P^{\max}/2$, and $P^{\max}/3$, where $P^{\max}$ ranged from 18 at high T to 90 at 300 K) to the asymptotic behavior

$$Q^{[P]}_{\mathrm{TT-FPI}}(T) = Q^{\mathrm{ESPE}}(T) + \frac{C_2(T)}{P^2} + \frac{C_3(T)}{P^3} \tag{3}$$

where $C_2(T)$ and $C_3(T)$ are fitting parameters, and $Q^{\mathrm{ESPE}}(T)$ is the final extrapolated value of the partition function at temperature T.

3. Computational Details

The potential energy surface (PES) used for the present set of calculations is the second of the two surfaces presented by Koput, Carter, and Handy (i.e., the fit presented in Table 3 of their paper,[23] which is the same surface that was used for their eigenvalue calculations). This PES is the same as the one used in our previous study[31] of H_2O_2. The functional form used for this fit does not account for the full permutational symmetry of the molecule; it is symmetric with respect to the exchange of the two OH groups, but not with respect to exchanges of just the two H atoms, nor with respect to exchanges of just the two O atoms. The symmetry number σ^{sym} for H_2O_2, D_2O_2, and $H_2{}^{18}O_2$ is 2 and for HOOD, $H^{18}OOH$, $D^{18}OOH$, and $H^{18}OOD$ is 1.

The masses of H, D, O, and ^{18}O are assumed to be 1.00782503, 2.01410178, 15.9949146, and 17.999160 amu, respectively. The zero of energy is at the minimum of the potential, which occurs for the configuration with $R_{\mathrm{OH}} = 0.96265$ Å (where R_{xy} is the distance from x to y), $R_{\mathrm{OO}} = 1.45248$ Å, HOO angles of 99.906°, and a dihedral angle of 112.456°. The value of the partition function depends on the zero of energy, which is often placed at the ground state. However, to calculate thermodynamic functions such as enthalpy of reaction or free energy of reaction from a potential energy surface, it is necessary to also calculate or include the zero-point energy, and therefore we calculate partition functions with the zero of energy at the equilibrium structure of the molecule, and this is the zero of energy used in the present article.

The numerical methods used for the TT-FPI calculations done in this paper are the same as in our previous work[31] on H_2O_2, and we limit ourselves to a few remarks. The calculations are performed in mass-scaled Jacobi coordinates, and the center-of-mass motion is removed. The path centroids are importance sampled using our recently presented approach[31] that employs independent ziggurat sampling[59,60] for six chosen coordinates—three Jacobi vector magnitudes and three Jacobi angles. Tight optimization of the domain-boundary parameters would yield negligible savings in computer time; therefore, conservative values are used. The importance-function width parameters used are the same as in our previous work,[31] and the importance-function center parameters are again taken to be the values at the equilibrium configuration. Because the coordinates used in the calculations depend on the masses, the numerical values of the center parameters also vary. The final parameters used in calculating the converged path-integral values for $Q^{[P]}_{\mathrm{TT-FPI}}(T)$ for the various isotopomers of H_2O_2 are given in Appendix 1 of Supporting Information. The classical ($P = 1$) results for any isotopolog may be obtained from the previous results for H_2O_2 via a simple mass-factor rescaling

$$Q^{P=1}_{m_a' m_b' m_c' m_d'}(T) = Q^{P=1}_{m_a m_b m_c m_d}(T) \left(\frac{m_a' m_b' m_c' m_d'}{m_a m_b m_c m_d} \right)^{3/2} \left(\frac{m_a + m_b + m_c + m_d}{m_a' + m_b' + m_c' + m_d'} \right) \tag{4}$$

If desired, all vibrational−rotational partition functions, $Q(T)$, in this paper could be converted to standard-state free energies, G_T°, by

$$G_T^\circ = -RT \ln \frac{Q^\circ_{\mathrm{trans}}(T) Q_{\mathrm{int}}(T)}{N_A} \tag{5}$$

where R is the gas constant, $Q^\circ_{\mathrm{trans}}(T)$ is the standard-state translational partition function, and N_{A} is Avogadro's number. Similarly, other thermodynamic functions could be obtained from $Q(T)$ by standard formulas. However we shall carry out the comparisons in terms of $Q(T)$ rather than G_T° or other thermodynamic functions.

4. Approximation Methods

4. A. Harmonic Approximation. The harmonic oscillator-separable rotation approximation to the vibrational−rotational partition function is

$$Q = Q_{\mathrm{rot}}\, e^{-\beta E_0^{\mathrm{HO}}} \tilde{Q}^{\mathrm{HO}} \tag{6}$$

where Q_{rot} is the rotational partition function, $\tilde{Q}^{\mathrm{HO}}$ is the harmonic oscillator (HO) approximation with the zero of energy temporarily at the ground state, given by

$$\tilde{Q}^{\mathrm{HO}} = \prod_{m=1}^{F} \frac{1}{1 - \mathrm{e}^{-\hbar\beta\omega_m}} \tag{7}$$

ω_m is the harmonic vibrational frequency of mode m, F is the

TABLE 1: Calculated Fundamentals and Harmonic Normal-Mode Frequencies[a] for $H^{18}OOH$, $H_2{}^{18}O_2$, HOOD, $D^{18}OOH$, $H^{18}OOD$, and D_2O_2

	$H^{18}OOH$	$H_2{}^{18}O_2$		HOOD		$D^{18}OOH$	$H^{18}OOD$	D_2O_2	
mode[b]	harm.[c]	harm.[c]	fund.[d]	harm.[c]	fund.[d]	harm.[c]	harm.[c]	harm.[c]	fund.[d]
ν_1	3795.6	3795.1	3611.0	2774.9	2675.2	2757.0	2774.9	2772.6	2676.3
ν_2	1434.2	1431.1	1391.5	1388.0	1349.5	1385.2	1384.6	1052.8	1027.6
ν_3	885.2	859.0	825.7	909.6	876.5	883.3	884.2	908.6	877.4
ν_4	381.2	380.4	369.7	334.7	313.9	333.9	333.9	279.4	254.2
ν_5	3808.5	3796.2	3613.5	3808.5	3622.9	3808.5	3795.6	2777.1	2675.6
ν_6	1326.4	1322.8	1262.5	1014.1	982.3	1010.3	1009.7	983.8	948.2

[a] As usual, we tabulate $\omega_m/2\pi c$ in cm^{-1} rather than ω_m in s^{-1}. [b] The vibrational modes are symmetric (ν_1) and antisymmetric (ν_5) OH stretches, symmetric (ν_2) and antisymmetric (ν_6) HOO bends, symmetric OO stretch (ν_3), and the HOOH torsion (ν_4). [c] The harmonic normal-mode frequencies as calculated using the POLYRATE v9.3 program.[68] [d] The calculated fundamentals as obtained by Koput, Carter, and Handy using their H_2O_2 potential energy surface.[24]

number of vibrational modes (six for all applications in the present article), and E_0^{HO} is the harmonic zero-point energy (ZPE) given by

$$E_0^{HO} = \frac{1}{2}\hbar\sum_{m=1}^{F}\omega_m \tag{8}$$

Another approximation is achieved by replacing the term E_0^{HO} in eq 6 with the accurate ZPE. This method is referred to as HO-Z, the zero-point-corrected harmonic oscillator approximation.

Note that the standard HO and classical (CHO) approximations are defined to include the harmonic approximation at only the one deepest minimum of the potential; this is a reasonable approximation for molecules such as ethane where, even though the torsion has three minima, they are quantum mechanically indistinguishable, and thus the quantum harmonic oscillator approximation correctly includes only one of them, but it is not reasonable for cases such as hydrogen peroxide where there is more than one contributing minimum. In such cases, a multiconformer (MC)-harmonic oscillator (HO)-rigid rotator (RR) approximation will be employed

$$Q^{MC-HO-RR} = \sum_i \exp(-\beta U_i) Q_i^{HO-RR} \tag{9}$$

where U_i denotes the difference between the energy of minimum i and the global minimum. (One could also define a classical version (MC-CHO-RR).) The sum in eq 9 includes only distinguishable minima; thus, for example, ethane and methanol would each have only one term because rotation of the methyl group leads to indistinguishable structures, whereas CH_2DOH would have three terms in eq 9. H_2O_2 has two isoenergetic distinguishable minima (they are stereoisomers) in the torsion coordinate, so the MC-HO-RR partition function is a factor of 2 larger than the HO-RR partition function.

The rotational partition function is evaluated in the quantum mechanical, symmetric top, rigid-rotor (RR) approximation, as discussed elsewhere.[31] (Alternative approximations to the rotational partition function change the result by only 2% or less, as shown in Appendix 2 of the Supporting Information.)

4. B. The Conventional Pitzer−Gwinn Approximation. The Pitzer−Gwinn[3,13,14,16,19] (PG) approximation can be used with the harmonic estimate of the zero-point energy (ZPE) to approximate the value of the anharmonic quantum mechanical vibrational partition function

$$Q^{PG} = e^{-\beta E_0^{HO}} Q_{CM}\left(\frac{\tilde{Q}^{HO}}{Q^{CHO}}\right) \tag{10}$$

TABLE 2: Comparison of Zero-Point Energies[a] from Various Sources

system	harmonic	from fundamentals[b]	accurate
H_2O_2	5838.4	5580.1	5726.1[b]
$H^{18}OOH$	5815.5	−	5704.1[c]
$H_2{}^{18}O_2$	5792.3	5537.0	5681.7[b]
HOOD	5114.9	4910.2	5028.8[b]
$D^{18}OOH$	5089.0	−	5003.5[c]
$H^{18}OOD$	5091.5	−	5006.0[c]
D_2O_2	4387.2	4229.7	4326.2[b]

[a] In cm^{-1}. [b] From the variational results of ref 61. [c] Present estimate.

where Q_{CM} is the anharmonic classical vibrational−rotational partition function, which we calculate by setting $P = 1$ in the path-integral algorithm, and Q^{CHO} is the classical mechanical harmonic oscillator approximation to the vibrational partition function, given by

$$Q^{CHO} = \prod_{m=1}^{F}\frac{1}{\hbar\beta\omega_m} \tag{11}$$

It is interesting to also consider a nonstandard version of the PG approximation. In this method, we employ the accurate value of the ZPE, called E_0, yielding

$$Q^{PG-Z} = e^{-\beta E_0} Q_{CM}\left(\frac{\tilde{Q}^{HO}}{Q^{CHO}}\right) \tag{12}$$

This approximation is interesting because E_0 can be calculated by quantum Monte Carlo methods[20,32] (or approximated in a variety of ways). Tables 1 and 2 give the harmonic vibrational frequencies and zero-point energies needed for the approximate calculations and compares them to fundamental[23,24,61] frequencies. (The frequencies for D_2O_2 and HOOD are in good agreement with available[62,63] experiments.)

When more than one minimum contributes significantly to the partition function, multiconformer analogues of eqs 10 and 12 could be used, where Q^{HO} is replaced by a weighted sum of quantum harmonic oscillators for all the distinguishable minima and Q^{CHO} is replaced by an analogous sum of classical partition functions. Note that the latter sum is not a strictly classical expression because the number of terms in the sum is governed by quantum mechanical consequences of symmetry. If all the contributing minima have identical Q^{HO-RR}, as in the present set of applications, the single- and multiconformer formulas would yield identical results, so we will not consider multiconformer PG approximations further here.

4. C. Generalized Pitzer−Gwinn Approximations. We will consider a very general extension of the Pitzer−Gwinn ap-

TABLE 3: TT-FPI-ESPE Partition Functions and 2σ Statistical Uncertainties for Various Temperatures

system	300 K	400 K	600 K	800 K
$H^{18}OOH$	$(7.018 \pm 0.062) \times 10^{-9}$	$(1.2081 \pm 0.0013) \times 10^{-5}$	$(3.0300 \pm 0.0025) \times 10^{-2}$	2.11323 ± 0.00091
$H_2{}^{18}O_2$	$(4.157 \pm 0.037) \times 10^{-9}$	$(6.9690 \pm 0.0075) \times 10^{-6}$	$(1.7078 \pm 0.0014) \times 10^{-2}$	1.18068 ± 0.00052
HOOD	$(2.322 \pm 0.011) \times 10^{-7}$	$(1.8128 \pm 0.0013) \times 10^{-4}$	0.21220 ± 0.00014	10.2992 ± 0.0037
$D^{18}OOH$	$(2.756 \pm 0.013) \times 10^{-7}$	$(2.0974 \pm 0.0015) \times 10^{-4}$	$(2.3934 \pm 0.0015) \times 10^{-1}$	11.5059 ± 0.0041
$H^{18}OOD$	$(2.735 \pm 0.013) \times 10^{-7}$	$(2.0868 \pm 0.0015) \times 10^{-4}$	$(2.3870 \pm 0.0015) \times 10^{-1}$	11.4862 ± 0.0041
D_2O_2	$(4.509 \pm 0.011) \times 10^{-6}$	$(1.56538 \pm 0.00070) \times 10^{-3}$	0.83431 ± 0.00042	27.9717 ± 0.0079

system	1000 K	1500 K	2400 K
$H^{18}OOH$	33.990 ± 0.026	2433.42 ± 1.55	165350 ± 170
$H_2{}^{18}O_2$	18.899 ± 0.015	1346.19 ± 0.86	91189 ± 84
HOOD	135.071 ± 0.091	7603.41 ± 4.04	449545 ± 368
$D^{18}OOH$	150.06 ± 0.10	8396.14 ± 4.63	493864 ± 595
$H^{18}OOD$	149.91 ± 0.10	8389.07 ± 4.38	494716 ± 423
D_2O_2	297.77 ± 0.17	13102.6 ± 6.41	671681 ± 624

proximation of the form

$$Q^{\mathrm{GPG}[P]}(T) = \frac{Q^{\mathrm{ref},P=\infty}(T)}{Q^{\mathrm{ref},P}(T)} Q^{[P]}(T) \tag{13}$$

where GPG denotes generalized Pitzer−Gwinn, $Q^{[P]}(T)$ is the path-integral partition function for some finite P, and $Q^{\mathrm{ref},P}(T)$ and $Q^{\mathrm{ref},P=\infty}(T)$ are the accurate quantum mechanical partition functions of some reference potential for this same value of P and for the infinite-P limit, respectively. If we choose our reference potential to be a sum of one-dimensional harmonic oscillators and set $P = 1$, we obtain the original PG approximation, and for any reasonable choice of reference potential, eq 13 converges to the accurate result as P is increased. For the rest of this paper, we will restrict consideration to reference potentials that are sums of harmonic oscillator functions, but we pause to remark that more general reference potentials, which partially account either for anharmonicity and/or intermode coupling, may prove to be more effective and would be a good subject for future investigation.

The finite-P quantum partition function for a harmonic oscillator can be expressed as[64]

$$Q^{\mathrm{HO},P}(T) = \frac{f^{P/2}}{f^P - 1} \tag{14}$$

where

$$f = 1 + \frac{R^2}{2} + \left(\frac{R}{2}\right)\sqrt{4 + R^2} \tag{15}$$

and

$$R = \frac{\hbar\beta\omega}{P} \tag{16}$$

The finite-P quantum partition function for a harmonic oscillator can also be expressed as[65]

$$Q^{\mathrm{HO},P}(T) = \frac{1}{[(\sqrt{1+\alpha^2} + \alpha)^P - (\sqrt{1+\alpha^2} - \alpha)^P]} \tag{17}$$

where

$$\alpha = \frac{\hbar\beta\omega}{2P} \tag{18}$$

If we use a reference potential of harmonic oscillators with frequencies ω evaluated from a Hessian at the global minimum of the potential, we shall refer to the results of eq 13 simply as GPG[P]. However, because the values of partition functions are very sensitive to the zero-point energy, we may be able to achieve higher accuracy for low P, if the reference function has a zero-point energy that is as close as possible to that of the accurate potential. One obvious way to achieve this (assuming the accurate ZPE is known) is simply to scale all of the harmonic frequencies using a single scale factor, i.e.,

$$\omega_i^{\mathrm{Z}} = \frac{E_0}{E_0^{\mathrm{HO}}} \omega_i \tag{19}$$

We will refer to this method as GPG-Z[P] where Z indicates frequency scaling based on the accurate zero-point energy.

4. D. Other Approximations. If we are not fortunate enough to know the accurate ZPE, we can use a known accurate value of $Q(T_o)$ at some temperature T_o to estimate an optimal scaling factor. This is done by numerically finding a scaling factor f_o that makes eq 13 hold exactly for $T = T_o$. In the $T_o \rightarrow 0$ limit, the optimal frequency-scaling factor will equal E_0/E_0^{HO}, and even at fairly high temperatures it will be close to this value. Because the path-integral calculations at moderate T values are quite affordable, performing a well converged calculation at one such temperature to estimate an approximate ZPE for use in GPG[P] calculations at lower temperatures can provide a considerable reduction in computational cost. This option is an interesting one for future study.

If one knows some of the higher-energy levels, one can define mixed methods that take advantage of this. This is illustrated in detail in Appendix 3 of the Supporting Information where we show how one can do better if one knows all the accurate fundamentals.

5. Results

5. A. Harmonic and Conventional PG Methods. Table 3 contains for several temperatures the values of $Q^{\mathrm{ESPE}}(T)$ and the 2σ statistical uncertainties, where σ denotes standard deviation, for the isotopomers considered here. (Intermediate results of these calculations are presented in Appendix 1 of the Supporting Information.) The small magnitudes of the 2σ statistical uncertainties given in Table 1 result partly from the highly effective importance-sampling scheme[31] and partly because the calculations used a large number $[(1 \times 10^7)-(2 \times 10^8)]$ of Monte Carlo samples.

Table 4 compares partition functions calculated with the MC-HO-RR approximation (with and without the accurate zero-point energy correction) and the two variants of the conventional PG

TABLE 4: Ratios of Approximate Partition Functions to the Accurate Path-Integral Results for Six Isotopologs at Various Temperatures

T(K)	system	HO-RR	MC-HO-RR	MC-HO-Z-RR	PG	PG-Z
300	H_2O_2	0.269	0.540	0.925	0.623	1.069
300	$H^{18}OOH$	0.271	0.543	0.926	0.627	1.070
300	$H_2{}^{18}O_2$	0.272	0.543	0.923	0.627	1.066
300	HOOD	0.301	0.601	0.908	0.694	1.048
300	$D^{18}OOH$	0.301	0.603	0.909	0.696	1.051
300	$H^{18}OOD$	0.302	0.603	0.909	0.696	1.049
300	D_2O_2	0.335	0.669	0.897	0.772	1.035
800	H_2O_2	0.363	0.727	0.890	0.852	1.042
800	$H^{18}OOH$	0.364	0.727	0.889	0.853	1.042
800	$H_2{}^{18}O_2$	0.364	0.728	0.888	0.856	1.041
800	HOOD	0.378	0.755	0.882	0.884	1.033
800	$D^{18}OOH$	0.377	0.755	0.881	0.887	1.032
800	$H^{18}OOD$	0.377	0.756	0.881	0.887	1.032
800	D_2O_2	0.393	0.784	0.875	0.918	1.024
2400	H_2O_2	0.398	0.797	0.852	0.952	1.020
2400	$H^{18}OOH$	0.398	0.795	0.850	0.958	1.020
2400	$H_2{}^{18}O_2$	0.398	0.795	0.850	0.953	1.019
2400	HOOD	0.402	0.804	0.847	0.964	1.016
2400	$D^{18}OOH$	0.403	0.805	0.847	0.966	1.016
2400	$H^{18}OOD$	0.402	0.804	0.846	0.964	1.015
2400	D_2O_2	0.406	0.813	0.843	0.973	1.010

approximation to the converged path-integral values. The MC-HO-RR approximation yields results that are systematically much too low, with errors ranging from 19% to 46%. The MC-HO-Z-RR approximation has errors ranging from 7% to 16%. The results for the PG-Z values are quite good, with errors of only 1% to 2% at 2400 K and 3.5% to 7% at 300 K. The errors are inversely proportional to the number of D atoms and, for a given number of D atoms, are inversely proportional to the number of ^{18}O atoms; this is consistent with the expectation of decreased quantum effects for heavier isotopes. The PG results are systematically too low (as expected because the harmonic ZPE overestimates the true ZPE), with errors ranging from 2.7% for D_2O_2 at 2400 K to 37.7% for H_2O_2 at 300 K, but the method still performs significantly better than the MC-HO-RR method.

We see that even where the errors of the approximate partition functions are large, they are often systematic; thus, it is interesting to examine the isotope effects. Table 5 shows values for the isotope effect, that is, the ratio of Q for H_2O_2 to Q for some isotopic molecule ($Q_{H_2O_2}/Q_{\text{isotopically substituted species}}$). Because the PG approximation only includes quantum effects at the harmonic level, and isotope effects are an inherently QM property, it yields isotope ratios that are identical to those of the HO-RR approximation. This may not be immediately obvious, but it can be readily shown by using eq 4 and the Teller−Redlich product rule[37,66,67]

$$\prod_{j=1}^{F}\frac{\omega_j}{\omega'_j}=\left(\frac{\sum_i m_i}{\sum_i m'_i}\right)\left(\frac{I_x I_y I_z}{I'_x I'_y I'_z}\right)^{1/2}\prod_i^{\#\text{atoms}}\left(\frac{m'_i}{m_i}\right)^{3/2} \tag{20}$$

where I_x, I_y, and I_z are the principle moments of inertia. The table includes the harmonic approximation, the HO-Z approximation, and the accurate path-integral results. It is interesting to see that the harmonic isotope effect for any species with one deuterium atom is off by 10−11% at 300 K. The isotope effect for the only species containing two deuterium atoms is off by 19% at 300 K, whereas any species without deuterium is only off by 1% at 300 K. At 2400 K, there is a similar trend although the errors are smaller and range from 0.2% to 2%. The HO-Z isotope effects are substantially more accurate than those of the HO calculations with the data for species with zero D atoms agreeing with accurate results within the statistical uncertainties, and results for species with one and two D atoms being accurate to within 1.7% and 3.1%, respectively.

B. Generalized Pitzer−Gwinn Approximation Results. In Table 6, we consider the convergence with respect to P of the GPG-Z[P] scheme for partition functions of H_2O_2 at 300 K—the lowest temperature and the lightest isotopomer considered here, and hence the hardest case to converge. The ESPE calculations were done with $P = 30$, 45, and 90 and involved an extrapolation correction of about 3.2%. The GPG[P] calculations are observed to converge rapidly and monotonically from above, with the $P = 30$ value already agreeing with the accurate result within the statistical uncertainties. The GPG-Z[P] calculations, which employ frequencies scaled to reproduce the accurate ZPE of 5726.1 cm^{-1}, display nonmonotonic convergence but provide outstanding accuracy for very low (2−5) P values. Figure 1 compares the correction factors, i.e., $Q^{\text{ref},[P=\infty]}(T)/Q^{\text{ref},[P]}(T)$, plotted as a ratio of the accurate value, for the two choices of reference potentials. The asymptotic convergence rate of the $Q^{[P]}(T)$ with increasing P is well characterized by using the unscaled harmonic frequencies, presumably because these characterize well the contribution from the stiffest, and thus slowest converging, region of the surface. The accurate ZPE is about 112.3 cm^{-1} below the harmonic value, due to anharmonicity effects that converge slowly with P; thus, at low P the GPG[P] scheme significantly underestimates the accurate partition function. By rescaling the frequencies to reproduce the accurate ZPE, the GPG-Z[P] scheme yields dramatically better results for low P values, with $P = 1$ giving errors of only ∼3% and the $P = 3$, 4, and 5 results, where the $Q^{[P]}(T)$ calculations begin to accurately treat the intermode coupling and low-frequency motions not represented by the reference potential, all being accurate to within 1%. For intermediate values of P, the path-integral calculations begin to account for significant portions of the anharmonicity in the high-frequency motions that the ZPE correction also approximately corrects for, and this double correction results in the GPG-Z[P] scheme predicting partition function estimates that are too high by as much as ∼3−4%. For larger P values, both schemes converge to the accurate result, but the GPG[P] scheme converges faster and is more accurate for $P > 10$.

In Tables 7 and 8, we consider partition functions for H_2O_2 and D_2O_2 calculated with the GPG-Z[P] scheme for P in the range of 1−4. The full range of temperatures is studied, and mean unsigned deviations (MUDs) between the accurate and approximate results over these seven temperatures are tabulated. The $P = 1$ results have an accuracy comparable to those of the PG-Z scheme and have MUDs from the accurate results of about 3−4%. Moving from $P = 1$ to $P = 2$ results in the MUDs being reduced by more than a factor of 2, to within 1.3−2.0%. The $P = 3$ results are dramatically better than the $P = 2$ results, with the $T \geq 800$ K data now being converged to within statistical uncertainties, having MUDs ranging from 0.4−0.9%. The $P = 4$ results have MUDs of 0.2−0.4% and provide excellent accuracy at all temperatures. As already mentioned, further increases in P can result in lower accuracy as the accurate path-integrals begin to converge anharmonic contributions that are already heuristically accounted for by the frequency scaling to reproduce the accurate ZPE, but in the large P limit the results converge to the accurate values.

TABLE 5: Accurate Path-Integral Results for $Q_{H_2O_2}/Q_{\text{isotopically substituted species}}$ and Percentage Errors in These Isotope Effects When They Are Calculated by the HO and HO-Z Approximations at Various Temperatures[a]

T(K)	$H^{18}OOH$	$H_2{}^{18}O_2$	HOOD	$D^{18}OOH$	$H^{18}OOD$	D_2O_2
			Accurate			
300	4.27(−1)	7.20(−1)	1.29(−2)	1.09(−2)	1.10(−2)	6.64(−4)
400	4.37(−1)	7.57(−1)	2.91(−2)	2.51(−2)	2.53(−2)	3.37(−3)
600	4.46(−1)	7.91(−1)	6.36(−2)	5.64(−2)	5.66(−2)	1.62(−2)
800	4.49(−1)	8.04(−1)	9.22(−2)	8.25(−2)	8.27(−2)	3.40(−2)
1000	4.52(−1)	8.12(−1)	1.14(−1)	1.02(−1)	1.02(−1)	5.16(−2)
1500	4.54(−1)	8.21(−1)	1.45(−1)	1.32(−1)	1.32(−1)	8.43(−2)
2400	4.55(−1)	8.24(−1)	1.67(−1)	1.52(−1)	1.52(−1)	1.12(−1)
			% Error in HO			
300	−0.6	−0.6	−10.2	−10.6	−10.6	−19.4
400	−0.4	−0.5	−7.9	−8.0	−8.0	−14.8
600	−0.2	−0.4	−5.0	−5.2	−5.2	−9.9
800	−0.1	−0.2	−3.8	−3.7	−3.8	−7.3
1000	−0.1	−0.2	−3.0	−3.0	−3.1	−5.8
1500	−0.1	−0.1	−1.9	−1.9	−2.0	−3.7
2400	0.2	0.2	−0.9	−1.0	−0.9	−2.0
			% Error in HO-Z			
300	−0.2	0.2	1.8	1.6	1.7	3.1
400	−0.1	0.1	1.2	1.3	1.3	2.4
600	0.0	0.0	1.1	1.1	1.1	1.9
800	0.1	0.1	0.9	1.0	0.9	1.7
1000	0.0	0.1	0.7	0.8	0.7	1.4
1500	0.0	0.1	0.6	0.7	0.6	1.1
2400	0.2	0.3	0.7	0.6	0.7	1.1

[a] Powers of 10 are in parentheses.

TABLE 6: Accurate Path-Integral and Generalized PG Path-Integral Results with Two Choices of the Reference Potential for the H_2O_2 Partition Function at $T = 300$ K[a]

P	$Q^{[P]}(T)$	$Q^{\text{GPG}[P]}(T)$	$Q^{\text{GPG}-\text{Z}[P]}(T)$
1	1.903(−2)[b]	1.866(−9)	2.869(−9)
2	1.563(−4)	2.046(−9)	2.906(−9)
3	9.423(−6)	2.188(−9)	2.926(−9)
4	1.486(−6)	2.321(−9)	2.961(−9)
5	4.055(−7)	2.325(−9)	2.983(−9)
6	1.588(−7)	2.544(−9)	3.032(−9)
7	7.824(−8)	2.629(−9)	3.055(−9)
8	4.522(−8)	2.683(−9)	3.055(−9)
9	2.971(−8)	2.750(−9)	3.077(−9)
10	2.123(−8)	2.795(−9)	3.084(−9)
15	8.259(−9)	2.933(−9)	3.095(−9)
20	5.510(−9)	2.973(−9)	3.074(−9)
30	3.984(−9)	2.991(−9)	3.039(−9)
45	3.409(−9)	2.993(−9)	3.015(−9)
90	3.092(−9)	2.992(−9)	2.997(−9)

[a] The converged result (obtained from an ESPE calculation) is (2.995 ± 0.013) × 10^{-9}. [b] Powers of 10 are in parentheses.

TABLE 7: Ratios of GPG-Z[P] Partition Functions for H_2O_2 to the Accurate Results

T	GPG-Z[1]	GPG-Z[2]	GPG-Z[3]	GPG-Z[4]
300	0.958	0.970	0.977	0.989
400	0.954	0.968	0.980	0.993
600	0.955	0.974	0.990	1.002
800	0.956	0.981	0.997	1.004
1000	0.957	0.984	0.998	1.002
1500	0.963	0.991	0.997	1.001
2400	0.971	0.994	0.999	1.000
MUD[a]	0.041	0.020	0.009	0.004

[a] Mean unsigned deviation from unity.

TABLE 8: Ratios of GPG-Z[P] Partition Functions for D_2O_2 to the Accurate Results

T	GPG-Z[1]	GPG-Z[2]	GPG-Z[3]	GPG-Z[4]
300	0.959	0.974	0.986	0.998
400	0.961	0.979	0.992	1.002
600	0.965	0.986	0.998	1.003
800	0.968	0.990	0.999	1.002
1000	0.971	0.992	0.999	1.000
1500	0.975	0.994	0.998	0.999
2400	0.981	0.995	0.998	0.999
MUD[a]	0.031	0.013	0.004	0.002

[a] Mean unsigned deviation from unity.

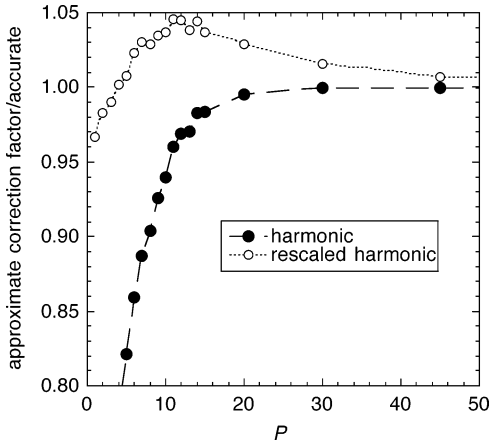

Figure 1. Ratio of the correction factors, $Q^{\text{ref},P=\infty}/Q^{\text{ref},P}$, to the accurate values for the GPG[P] (harmonic reference potential) and GPG-Z[P] (scaled harmonic reference potential) schemes as a function of P at $T = 300$ K.

In Table 9, we consider the H_2O_2/D_2O_2 isotope effect, which is the hardest test case, calculated using the GPG-Z[P] scheme for P in the range of 1−4. As in the case of the harmonic results, the isotope effects benefit from cancellation of systematic errors in the absolute partition functions and even the $P = 1$ results have MUDs of 1% or below. The results for $P = 2-4$ are all very close to the ESPE benchmarks.

In Table 10, we consider estimates of the accurate ZPE of H_2O_2, obtained using various values of T and P using the GPG-Z[P] scheme. Specifically, we determine the ZPE we would need to scale the harmonic frequencies for the GPG-Z[P] method to reproduce the $Q^{\text{ESPE}}(T)$ result for a given value of T and P.

TABLE 9: Ratios of GPG-Z[*P*] H_2O_2/D_2O_2 Isotope Ratios to the Accurate Results

T	GPG-Z[1]	GPG-Z[2]	GPG-Z[3]	GPG-Z[4]
300	0.998	0.997	0.991	0.990
400	0.993	0.989	0.987	0.991
600	0.990	0.988	0.992	0.999
800	0.988	0.991	0.998	1.002
1000	0.986	0.992	1.000	1.002
1500	0.987	0.996	0.999	1.002
2400	0.990	0.999	1.001	1.001
MUD[a]	0.010	0.007	0.005	0.004

[a] Mean unsigned deviation from unity.

TABLE 10: Approximate ZPE Estimates Obtained from the GPG-Z[*P*] Scheme for H_2O_2[a]

T	$P = 1$	$P = 2$	$P = 3$	$P = 4$
300	5717.2 ± 1.2	5720.5 ± 2.2	5722.3 ± 3.7	5726.4 ± 3.9
400	5711.5 ± 0.5	5715.3 ± 0.8	5719.4 ± 1.3	5727.4 ± 2.0
600	5700.0 ± 0.7	5707.7 ± 1.4	5720.6 ± 2.2	5737.1 ± 3.2
800	5687.0 ± 0.6	5702.9 ± 1.4	5725.7 ± 2.2	5749.0 ± 3.2
1000	5671.6 ± 1.7	5694.8 ± 3.8	5726.9 ± 6.4	5749.5 ± 9.8
1500	5629.5 ± 2.9	5678.6 ± 7.0	5706.6 ± 14	5742 ± 21
2400	5541.6 ± 9.5	5634 ± 30	5691 ± 56	5734 ± 91

[a] The accurate and harmonic ZPEs are 5726.1 and 5838.4 cm^{-1}, respectively.

We provide uncertainty estimates by considering the two cases where the $Q^{ESPE}(T)$ and $Q^{[P]}(T)$ values are shifted in opposite directions by their 2σ statistical uncertainties. As $T \rightarrow 0$, the results will all converge to the accurate ZPE. As P is increased, for finite T, the ZPE estimates all increase and presumably become close to the harmonic ZPE, but for small values of P, the values will lie closer to the accurate ZPE for the reasons already discussed above. For the present system, $P = 3$ yields the best estimates. Even at moderately high temperatures, the ZPE estimates are quite good and may prove useful for use in GPG-Z[*P*] calculations at lower temperature (where the calculations are significantly more expensive) if more accurate means of estimating the ZPE are not feasible.

6. Conclusions

This paper presents converged accurate quantal rovibrational partition functions for six isotopically substituted hydrogen peroxides. The calculations are carried out by the TT-FPI-ESPE path-integral method, and the 2σ statistical errors are only about 0.1% from 400 to 2400 K. At the lowest temperature calculated (300 K), where the calculations are the most difficult, the statistical error is no more than 0.9% for all species examined here.

These well-converged results allow us to compare approximate methods such as the harmonic oscillator and Pitzer−Gwinn (PG) methods. At 300 K, we find that the error for the PG result when compared to the accurate path-integral results ranges from 23 to 38%, and at 2400 K the percent error ranges from 2 to 5%. This is a large improvement over the errors in the multiconfiguration harmonic approximation, which ranges from about 46% at 300 K to 20% at 2400 K.

For isotope effects, the harmonic approximation errors at 300 K ranged from 10 to 19% for those systems with deuterium and are about 1% for those systems without a deuterium atom. At the highest temperature considered, the errors for all species were at most 2%.

We presented a general scheme for quantum mechanical generalizations of the Pitzer−Gwinn approximation that may be systematically extended until they converge to the accurate result by increasing the number, P, of path expansion parameters (discretized points in the present set of calculations) used. Those schemes that account for the zero-point energy (ZPE) accurately yield well-converged results with P in the range of 2−4 even at the lowest temperatures considered. When no ZPE estimates are available, and only the harmonic reference potential is considered, the GPG[*P*] scheme still converges to the accurate result much more rapidly than the TT-FPI calculations do. These methods can also be used to get reasonable and affordable approximations of the accurate zero-point energy. More refined reference potentials than the simple harmonic ones considered here may prove substantially more effective for both the calculation of accurate partition functions and ZPE estimates; this is an enticing topic for future research.

In addition to the tests reported in this paper, the converged results presented here should be useful as benchmarks for testing all kinds of future approximations. They should be especially useful because of the high precision and wide temperature range and because there are so few converged partition function calculations available[30] for real molecules with four or more atoms; in fact, this paper increases the number of cases from two[30,31] to eight.

Acknowledgment. This work was supported in part by the National Science Foundation under Grant No. CHE03-49122.

Supporting Information Available: Parameters for converged path-integral calculations and tables of the partition functions for $P = 1$, $P = 2$, $P = 3$, $P = 4$, $P^{max}/3$, $P^{max}/2$, P^{max}, and Q^{ESPE}; a table of the moments of inertia and tables of the rotational partition functions; tables of nonstandard and generalized Pitzer−Gwinn approximations for PG-F and GPG-ZF. This material is available free of charge via the Internet at http://pubs.acs.org.

References and Notes

(1) Kassel, L. S. *Chem. Rev.* **1936**, *18*, 277.
(2) Darling, B. T.; Dennison, D. M. *Phys. Rev.* **1940**, *57*, 128.
(3) Pitzer, K. S.; Gwinn, W. D. *J. Chem. Phys.* **1942**, *10*, 428.
(4) Nielsen, H. H. *Handb. Phys.* **1959**, *37/1*, 173.
(5) Wooley, H. W. *J. Res. Natl. Bur. Stand. (U.S.)* **1956**, *56*, 105.
(6) Bron, J.; Wolfsberg, M. *J. Chem. Phys.* **1962**, *57*, 2862.
(7) Morino, Y.; Kuchitsu, K.; Yamamoto, S. *Spectrochim. Acta* **1968**, *24A*, 335.
(8) Whitehead, R. J.; Handy, N. C. *J. Mol. Spectrosc.* **1975**, *55*, 356.
(9) Mills, I. M. In *Molecular Spectroscopy*; Rao, K. N., Mathews, C. W., Eds.; Academic: New York; p 115.
(10) Carney, G. C.; Sprandel, L. L.; Kern, C. W. *Adv. Chem. Phys.* **1978**, *37*, 305.
(11) Bowman, J. M. *J. Chem. Phys.* **1978**, *68*, 608.
(12) Thompson, T. C.; Truhlar, D. G. *Chem. Phys. Lett.* **1980**, *75*, 87.
(13) Isaacson, A. D.; Truhlar, D. G.; Scanlon, K.; Overend, J. *J. Chem. Phys.* **1981**, *75*, 3017.
(14) Isaacson, A. D.; Truhlar, D. G. *J. Chem. Phys.* **1981**, *75*, 4090.
(15) Bohmann, J.; Witschel, W. *Z. Naturforsch., A: Phys. Sci.* **1983**, *38*, 167.
(16) Isaacson, A. D.; Truhlar, D. G. *J. Chem. Phys.* **1984**, *80*, 2888.
(17) Roger, A. *Chem. Phys. Lett.* **1985**, *119*, 290.
(18) Tucker, S. C.; Thompson, T. C.; Lauderdale, J. G.; Truhlar, D. G. *Comput. Phys. Commun.* **1988**, *51*.
(19) Truhlar, D. G.; Isaacson, A. D. *J. Chem. Phys.* **1991**, *94*, 357.
(20) Suhm, M. A.; Watts, R. O. *Phys. Rep.* **1991**, *204*, 293.
(21) Carter, S.; Bowman, J. M.; Handy, N. C. *Theor. Chem. Acc.* **1998**, *100*, 191.
(22) Isaacson, A. D. *J. Chem. Phys.* **1998**, *108*, 9978.
(23) Koput, J.; Carter, S.; Handy, N. C. *J. Phys. Chem. A* **1998**, *102*, 6325.
(24) Koput, J.; Carter, S.; Handy, N. C. *J. Chem. Phys.* **2001**, *115*, 8345.
(25) Manthe, U.; Huarte-Larrañaga, F. *Chem. Phys. Lett.* **2001**, *349*, 321.
(26) Mielke, S. L.; Truhlar, D. G. *J. Chem. Phys.* **2001**, *115*, 652.
(27) Miller, T. F., III; Clary, D. C. *J. Chem. Phys.* **2002**, *116*, 8262.
(28) Miller, T. F., III; Clary, D. C. *J. Chem. Phys.* **2003**, *119*, 68.

(29) Glaesemann, K. R.; Fried, L. E. *J. Chem. Phys.* **2003**, *118*, 1596.
(30) Chakraborty, A.; Truhlar, D. G.; Bowman, J. M.; Carter, S. *J. Chem. Phys.* **2004**, *121*, 2071.
(31) Lynch, V. A.; Mielke, S. L.; Truhlar, D. G. *J. Chem. Phys.* **2004**, *121*, 5148.
(32) McCoy, A. B.; Huang, X.; Carter, S.; Landeweer, M. Y.; Bowman, J. M. *J. Chem. Phys.* **2005**, *122*, 061101.
(33) Harding, L. B. *J. Phys. Chem.* **1989**, *93*, 8004.
(34) Feynman, R. P. *Statistical Mechanics: A Series of Lectures*; Benjamin: Reading, MA, 1972.
(35) Feynman, R. P.; Hibbs, A. R. *Quantum Mechanics and Path Integrals*; McGraw-Hill: New York, 1965.
(36) Wilson, E. B., Jr. *Chem. Rev.* **1940**, *27*, 17.
(37) Herzberg, G. *Infrared and Raman Spectra*; D. Van Nostrand: Princeton, 1945.
(38) Miller, W. H. *J. Chem. Phys.* **1975**, *63*, 1166.
(39) Doll, J. D.; Freeman, D. L. *J. Chem. Phys.* **1980**, *80*, 2239.
(40) Schulman, L. S. *Techniques and Applications of Path Integration*; Wiley: New York, 1981.
(41) Coalson, R. D. *J. Chem. Phys.* **1986**, *85*, 926.
(42) Coalson, R. D.; Freeman, D. L.; Doll, J. D. *J. Chem. Phys.* **1986**, *85*, 4567.
(43) Doll, J. D.; Coalson, R. D.; Freeman, D. L. *Phys. Rev. Lett.* **1986**, *55*, 1.
(44) Freeman, D. L.; Doll, J. D. *Adv. Chem. Phys.* **1988**, *70B*, 139.
(45) Coalson, R. D.; Freeman, D. L.; Doll, J. D. *J. Chem. Phys.* **1989**, *91*, 4242.
(46) Doll, J. D.; Freeman, D. L.; Beck, T. *Adv. Chem. Phys.* **1990**, *78*, 61.
(47) Topper, R. Q.; Truhlar, D. G. *J. Chem. Phys.* **1992**, *97*, 3647.
(48) Topper, R. Q.; Tawa, G. J.; Truhlar, D. G. *J. Chem. Phys.* **1992**, *97*, 3668.
(49) Topper, R. Q.; Zhang, Q.; Liu, Y.-P.; Truhlar, D. G. *J. Chem. Phys.* **1993**, *98*, 4991.
(50) Kleinert, H. *Path Integrals in Quantum Mechanics, Statistics, and Polymer Physics*, 2nd ed.; World Scientific: Singapore, 1995.
(51) Mielke, S. L.; Srinivasan, J.; Truhlar, D. G. *J. Chem. Phys.* **2000**, *112*, 8758.
(52) Srinivasan, J.; Volobuev, Y. L.; Mielke, S. L.; Truhlar, D. G. *Comput. Phys. Commun.* **2000**, *128*, 446.
(53) Mielke, S. L.; Truhlar, D. G. *J. Chem. Phys.* **2001**, *114*, 621.
(54) Predescu, C.; Doll, J. D. *J. Chem. Phys.* **2002**, *117*, 7448.
(55) Predescu, C.; Doll, J. D. *Phys. Rev. E: Stat. Phys., Plasmas, Fluids, Relat. Interdiscip. Top.* **2003**, *67*, 026124.
(56) Predescu, C.; Sabo, D.; Doll, J. D. *J. Chem. Phys.* **2003**, *119*, 4641.
(57) Kleinert, H. *Path Integrals in Quantum Mechanics, Statistics, Polymer Physics, and Financial Markets*, 3rd ed.; World Scientific: Singapore, 2004.
(58) Mielke, S. L.; Truhlar, D. G. *Chem. Phys. Lett.* **2003**, *378*, 317.
(59) Marsaglia, G.; Tsang, W. W. *J. Sci. Stat. Comput.* **1984**, *5*, 349.
(60) Marsaglia, G.; Tsang, W. W. *J. Stat. Software* **2000**, *5*.
(61) Koput, J. Private communication.
(62) Khachkuruzov, G. A.; Przhevalskii, I. N. *Opt. Spectrosc.* **1977**, *41*, 323.
(63) Bain, O.; Giguere, P. A. *Can. J. Chem.* **1955**, *33*, 527.
(64) Schweizer, K. S.; Stratt, R. M.; Wolynes, P. G. *J. Chem. Phys.* **1981**, *75*, 1347.
(65) Takahashi, M.; Imada, M. *J. Phys. Soc. Jpn.* **1984**, *53*, 3765.
(66) Redlich, O. *Z. Phys. Chem.* **1935**, *28*, 371.
(67) Wilson, E. B.; Decius, J. C.; Cross, P. C. *Molecular Vibrations*; McGraw-Hill Book Company: New York, 1955.
(68) Corchado, J. C.; Chuang, Y.-Y.; Fast, P. L.; Villà, J.; Hu, W.-P.; Liu, Y.-P.; Lynch, G. C.; Nguyen, K. A.; Jackels, C. F.; Melissas, V. S.; Lynch, B. J.; Rossi, I.; Coitiño, E. L.; Fernandez-Ramos, A.; Pu, J.; Albu, T. V.; Steckler, R.; Garrett, B. C.; Isaacson, A. D.; Truhlar, D. G. POLYRATE, version 9.3, University of Minnesota, Minneapolis, 2003.